Hindawi
Security and Communication Networks
Volume 2022, Article ID 5362928, 10 pages
https://doi.org/10.1155/2022/5362928

Research Article

An Experimental and Modeling Study on the Combustion of Gasoline-Ethanol Surrogates for HCCI Engines

Peng Yin,[1] Wenfu Liu,[1] Yong Yang,[1] Haining Gao,[1] and Chunhua Zhang[2]

[1]*School of Energy Engineering, Huanghuai University, Zhumadian,463000, China*
[2]*School of Automobiles, Chang'an University, Xi'an 710064, China*

Correspondence should be addressed to Chunhua Zhang; 2017022008@chd.edu.cn

Received 15 January 2022; Revised 25 January 2022; Accepted 27 January 2022; Published 21 February 2022

Academic Editor: Thippa Reddy G

Copyright © 2022 Peng Yin et al. This is an open access article distributed under the Creative Commons Attribution License, which permits unrestricted use, distribution, and reproduction in any medium, provided the original work is properly cited.

As an effective clean fuel, ethanol has the characteristics of improving antiknock quality and reducing emissions. It is an ideal antiknock additive for Homogeneous Charge Compression Ignition (HCCI) engines. The oxidation of gasoline-ethanol surrogates in HCCI engines is a very complex process which is dominated by the reaction kinetics. This oxidation process directly determines the performance and emissions of HCCI engines. Coupling the computational fluid dynamic (CFD) model with the gasoline-ethanol surrogate mechanism can be used for fuel design, so the construction of a reduced mechanism with high accuracy is necessary. A mechanism (278 species, 1439 reactions) at medium and low temperatures and experiments in a HCCI engine for the oxidation of gasoline-ethanol surrogates were presented in this paper. Directed relation graph with error propagation (DRGEP) method and quasi-steady-state assumption (QSSA) method were used in order to get a reduced model. Then, the kinetics of the vital reactions related to the formation and consumption of H and OH were adjusted. To validate the model, the HCCI experiments for the oxidation of gasoline-ethanol surrogates were conducted under different operating conditions. The verification result indicated that the present model can predict the oxidation process of gasoline-ethanol effectively.

1. Introduction

Due to rapid urbanization and industrialization, pollution levels are increasing at an alarming rate recently. Processing the fuel efficiently plays an important role in reducing the pollution due to fuel emissions, which can play an important role in improving the health of the citizens, especially in urban areas. Gasoline-ethanol is a multicomponent substance of thousands of macromolecular hydrocarbons and it is time-consuming and costly to develop a mechanism for the real fuel. Moreover, the application of the detailed model for complex gasoline-ethanol surrogate fuels in HCCI engine simulations is not practical with current computing resources, due to the large scale and the stiffness of the detailed mechanism. Therefore, the representative components of gasoline should be selected reasonably and the model of multicomponent gasoline surrogates should be reduced while maintaining its good performance.

Primary reference fuel (PRF), the two-component (iso-octane/n-heptane) mixture, is generally considered to be the most common surrogates for gasoline. In recent years, more and more experiments were conducted in HCCI engines under high pressure, medium and low temperatures, and low equivalent ratio conditions, which provided a basis for the application of PRF mechanism in HCCI engine simulations. The PRF oxidation process of "the first oxygen addition ⟶ the first isomerization ⟶ the second oxygen addition ⟶ the second isomerization" is the key section during the autoignition process. In addition, as a commonly used additive, ethanol has become an important component for gasoline surrogate fuels due to its good antiknock performance and low emissions. The chemical kinetic mechanism of ethanol-PRF coupled with CFD software helps to understand the oxidation phenomena of mixture such as autoignition, flame propagation, flameout, combustion stability, and emissions. This is of great importance for

further improving combustion efficiency and reducing emissions.

The PRF models given by Halstead et al. [1] and Cox and Cole [2] were empirical models, which were still widely applied in the simulation of autoignition process. Then Li et al. [3] proposed a reduced model for predicting PRF oxidation behaviors, including ignition delay (τ), heat release rate (*HRR*), and molarity of vital species. This model can well predict the oxidation behaviors of PRF in the low and medium temperature, but the predictions at high temperature phase were not satisfactory. The reduced mechanism developed by Tanaka et al. [4] can be applicable for predicting τ, *HRR*, and knock in HCCI engines in a wide range, but it was difficult to predict the emission characteristics. However, the PRF mechanism constructed [5] by using the hierarchical expansion method can be used to calculate emissions of PHAs and other pollutants, although it was not accurate in predicting τ under the intake temperature (T_{in}) range of 300 K ~ 434 K and the pressure (P) of 4.0 MPa.

The model of Curran et al. [6] can well predict the ignition process on a wider scale of T_{in}s, Ps, and φs. According to the model [6], Ra and Reitz [7] proposed a reduced model, involving 41 species and130 reactions, which may predict in-cylinder pressure (P), τ, and *HRR* accurately. Then, in order to solve the problem of cross-reactions, Kirchen et al. [8] added the cross-reactions to the models of Tanaka et al. [4] and Marinov [9]. In 2013 and 2015, two mechanisms developed by Liu et al. [10] and Wang et al. [11] were also presented for the combustion of gasoline surrogates.

A detailed three-component (iso-octane/n-heptane/ethanol) model [12] may predict laminar flame speeds (S_Ls) accurately under high temperature. Then Zheng and Zhong [13] developed a reduced three-component model (50 species, 193 reactions). Its calculated τs were highly consistent with the experimental values. Based on this model, a three-component model [14] was proposed by adding some elementary reactions related to H and updating relevant kinetic parameters, which can predict S_Ls and τs accurately. Moreover, Lemaire et al. [15] analyzed the effect of the additive (ethanol) to gasoline on the formation of soot. They pointed out that adding 10% ~ 30% (by volume) ethanol can reduce the production of soot precursor significantly; the amount of reduction for soot was 25% ~ 81%. In 2019, Li et al. [16] developed a highly reduced four-component gasoline-ethanol model, which may predict the experimental data for PRF, toluene primary reference fuel (TRF), and PRF-ethanol surrogates.

In recent years, we have conducted in-depth studies on the HCCI test and chemical reaction kinetics of related mixtures (Energy, 2019, 169:572–579. Tehnički Vjesnik Technical Gazette, 2020, 27(5):1571–1578. (SCI); Acta Microscopica, 2020, 29(2):720–731. (SCI)). In the field of chemical reaction kinetics, the mechanism of linear alkane and iso-alkanes and the chemical reaction kinetics of paraffin fuels have been constructed. In addition, preliminary achievements have been made in the research of primitive reactions and active groups sensitive to ignition delay.

In summary, the combustion process of gasoline-ethanol blend has attracted more and more attention recently. Many gasoline-ethanol mixture mechanisms have been constructed. However, due to the stiffness caused by long simulation time scale, the existing models are too large in scale and have poor accuracy under the current computing resources. Furthermore, HCCI validation experiments fueled with a hydrocarbon blend or a hydrocarbon-oxygen blend are rare and more experimental data is needed to compare with the calculated value, in order to further verify the reduced model. Therefore, the objective of this paper is to perform HCCI experiments on the combustion of gasoline-ethanol surrogates and to develop a smaller size mechanism for the lean gasoline-ethanol surrogates ($\varphi < 1$) by implementing a reduction and merge scheme using DRGEP and QSSA methods. In order to carry out extensive validation of this reduced model, not only the calculation used by the proposed model should be compared with the results of the HCCI experiments, but also the new model should be compared with the previous literature models.

2. Kinetic Modeling

In this section, the processes of the initial mechanism construction, the automatic chemistry mechanism reduction for gasoline-ethanol surrogates, and the determination of the final mechanism are presented, as displayed in Figure 1. The reduced gasoline-ethanol mechanism was constructed by first reducing and then merging.

Firstly, in order to get a mechanism of smaller size, DRGEP method was used to eliminate the insignificant species efficiently, and QSSA method was used to identify the species that were in quasi-steady-state. Following the above process, the two submechanisms (the models of ethanol [9] and PRF [6]) were reduced. Taking the reduction of PRF submechanism as an example, according to the PRF reaction path given by Ra and Reitz [7], initial reactants (iso-octane/n-heptane/O_2), intermediate components (C_2H_3, CH_3, CH_2CHO), and final products (CO_2, H_2O) were selected as target substances. The larger the error threshold was set, the smaller the reduced mechanism scale would be and the prediction accuracy would decrease. In the process of reduction, a smaller threshold is set and reduction is carried out several times to ensure the prediction accuracy. Subsequently, a powerful and accurate merge for the reduced submechanisms from three disparate fuels was conducted.

Secondly, several relevant reactions involving H and OH in the products or reactants were revised, and the parameters of these reactions were adjusted. Finally, the final mechanism (278 species and 1439 reactions) was proposed.

Thirdly, the repeated reactions and components of PRF and ethanol mechanisms are mainly small molecule reactions of C_1~C_3, H, and O_2. However, rate constants of the same reactions in these two mechanisms are different, leading to great changes in the generation or consumption rates of many free radicals (H, OH, H_2O_2, HO_2, etc.). The rate constants of the small molecular reactions of C_1~C_3, H, and O_2 in PRF submechanism were selected.

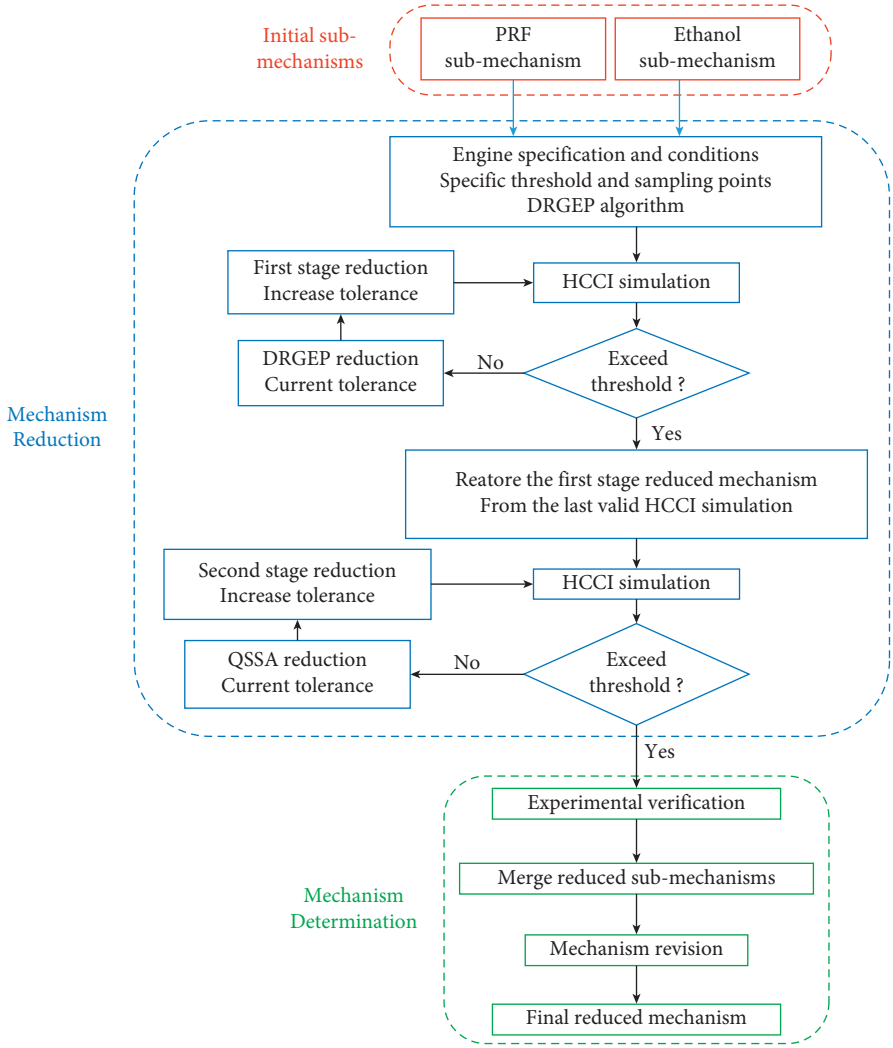

Figure 1: Flowchart of mechanism construction.

2.1. Base Mechanism and Case Settings. In order to keep the consistency between predictions and experimental results on reaction rate, transport, and thermodynamic data, the detailed chemical kinetic mechanism of PRF (1034 species, 4236 reactions) [6] and the semidetailed ethanol model (57 species, 383 reactions) [9] were taken as base mechanisms.

Mechanism [6] has been used in the simulations of HCCI engines in [17, 18]. The ethanol submechanism has been validated by comparing with the experimental S_Ls and τs. The predictions by ethanol submodel were also compared with mole fractions of species measured in stirred and flow reactors. In this paper, by combining complex calculation with recently obtained rate constants, the ethanol submechanism was updated by adjusting the Arrhenius coefficients of some elementary reactions, as shown in Table 1 and [19–22].

The reduction work of the mechanism for gasoline-ethanol surrogates was carried out on the conditions targeted for HCCI engines. HCCI engines generally operate at low φs, so the flame temperature should be lower compared with conventional internal combustion engines. To reduce the chemical model, 18 conditions were chosen at different temperatures (500 K~1000 K) and different φs (0.25, 0.3 and 0.5). The three-component fuel (iso-octane/n-heptane/ethanol = 62%: 18%: 20% by volume) should be considered as a substitute for ethanol-gasoline fuels [23], and it was used as gasoline-ethanol surrogates in this paper.

All the related calculations were performed by using CHEMKIN package. Assuming that mass transport is infinitely fast, the gas phase reaction is controlled solely on the nature of each species, not by transport constraints. The whole domain has uniform thermodynamic and transport properties.

For nonadiabatic cases, heat transfer between the cylinder and the wall was noticed. Related parameters of heat transfer were set according to the Woschni formula [24]. The relevant data in the model were set according to the specification of the test engine bench and the running conditions. Specifications for the test engine were presented by Zhang and Wu [25].

2.2. Mechanism Reduction. The reduction of the mechanism was implemented by DRGEP and QSSA approaches.

The DRGEP method is used for initial reduction. For a detailed mechanism, when specific species (reactants, reaction

Table 1: Updated reactions for ethanol.

Reaction	A	n	E	Reference
$C_2H_5OH + OH = C_2H_4OH + H_2O$	6.20E3	2.7	−576	[17]
$C_2H_5OH + OH = CH_3CHOH + H_2O$	1.31E5	2.4	−1457	[17]
$C_2H_5OH + H = C_2H_4OH + H_2$	1.88E3	3.2	7150	[16]
$C_2H_5OH + H = CH_3CHOH + H_2$	1.79E5	2.5	3420	[16]
$C_2H_5OH + O = C_2H_4OH + OH$	9.69E2	3.2	4658	[19]
$C_2H_5OH + O = CH_3CHOH + OH$	1.45E5	2.4	876	[19]
$C_2H_5OH + O = CH_3CH_2O + OH$	1.46E-3	4.7	1727	[19]
$C_2H_5OH + CH_3 = C_2H_4OH + CH_4$	3.30E2	3.3	12291	[18]
$C_2H_5OH + CH_3 = CH_3CHOH + CH_4$	1.99E1	3.4	7635	[18]
$C_2H_5OH + CH_3 = CH_3CH_2O + CH_4$	2.04	3.6	7722	[18]

products, and important intermediate species) are set as the target component, then a series of species are strongly coupled to the target component. When an error threshold is set, DRGEP method can identify unimportant components and thus remove those components and the reactions associated with them. The DRGEP method was implemented efficaciously by removing the species and reactions whose target variable error in the worst case exceeds the threshold. The worst-case error was considered to be the maximum relative error of the original and reduced mechanisms in the 24 target cases. When the worst-case error was within the threshold, the tolerance would be increased and the first stage reduction would continue. The reduction of the first phase was terminated until the worst-case error of simulation results exceeded the preset threshold (5%). At this stage, some species (ethanol, i-C_8H_{18}, n-C_7H_{16}, s-C_2H_4OH) was chosen to be the starting species. Relative tolerance of mole-fractions for CO, CO_2, and H was 0.009, respectively, and threshold for iso-octane, s-C_2H_4OH, CH_3CHO, n-heptane, and ethanol was set to 5%, respectively. After reduction, the first-stage model (296 species, 1691 reactions) was developed.

Subsequently, QSSA method was also applied. The QSSA method [26–28] can be used to identify some intermediate species whose production and consumption rates were nearly equal. For these species, the change in concentration was almost negligible. After setting a threshold, these intermediate quasi-steady-state (QSS) species would be processed by a nonlinear algebraic system. In this paper, the relative tolerances of *HRR* and ignition delay were set to 0.1 compared with the initial mechanism; the relative tolerance of mole fractions for CO, iso-octane, and n-heptane were set to 7%. iC_4H_8 and C_5H_3 were identified under quasi-steady-state. It not only saved computational time, but also greatly reduced the stiffness of the ordinary differential equation system. After second-stage reduction, the model (277 species, 1437 reactions) was constructed.

3. Experimental Setting

In this paper, the HCCI experiments were performed to validate the mechanism of gasoline-ethanol surrogates and to provide more basic data on combustion characteristics of the test fuel. The three-component fuel (iso-octane/n-heptane/ethanol = 62%: 18%: 20% by volume) (a surrogate for 95 RON gasoline) was used as the test fuel in HCCI experiments. The selected HCCI operating conditions are shown in Table 2.

Table 2: HCCI operating conditions.

Test	n (r/min)	φ	T_{in} (K)	Fuel quantity per cycle (mg/cyc)
OP1	1200	0.3	433	11.19
OP2	1200	0.3	423	11.45
OP3	1200	0.3	413	11.74
OP4	1200	0.3	403	12.03
OP5	1200	0.3	393	12.35
OP6	1200	0.4	433	15.66
OP7	1200	0.4	423	16.04
OP8	1200	0.4	413	16.43
OP9	1200	0.4	403	16.85
OP10	1200	0.4	423	17.29
OP11	1200	0.35	423	13.19
OP12	1200	0.25	393	10.29

3.1. Experimental Setup. The test engine was retrofitted based on a water cooled, direct injection, naturally aspirated, original engine, CT2100Q. The first cylinder maintained the conventional diesel engine mode, while the second cylinder operated in HCCI mode.

In order to meet the requirements of HCCI operating mode, the intake system, exhaust system, and fuel system were modified. The details and schematic of the test HCCI engine system can be found in [25]. In order to control the intake temperature (T_{in}), an independent port-fuel-injection system and an electric heating system were installed on the second intake pipe. When the injection pulse width was bigger than 2.5 milliseconds, the test fuel was injected into the HCCI cylinder. The injection timing was set to 30°CA BTDC and duration can vary from 5 milliseconds to 8 milliseconds under different operating conditions. The P of the second cylinder was recorded by Kistler 6052A. This piezoelectric pressure makes it possible to record digital signals (TTL: >4, 5 V high, <1 V low level). These signals are then transmitted, either by ECU or statically from the test cylinder, and then it was analyzed by Kibox 283A. The accuracy for the instruments employed can be seen in [25].

3.2. Experimental Procedure. To start the test engine in HCCI mode smoothly, at the beginning, the engine worked in diesel mode. When the water temperature reached 95°C and oil temperature reached 85°C, the diesel supply to the first cylinder was stopped and the fuel injection for the other cylinder was started simultaneously. As a result, the operating mode was successfully switched. When the HCCI

engine run stably, the in-cylinder pressures were recorded, averaged, and analyzed based on 100 consecutive cycles.

4. Results and Discussion

τ, S_L, *HRR*, *P*, and molarity for vital species are the key parameters of the prediction.

4.1. Laminar Flame Speed. The simulation analysis was performed in flame speed reactor. Figure 2 gives S_Ls of three single-component fuels at $T_{in} = 298$ K and $P_{in} = 0.1$ MPa. The comparison of S_Ls between the results of calculation obtained by using the second-stage model and experimental results under different φs can be seen in Figure 2(a). It can be found that the trends of the calculated S_Ls with φs are consistent with the experimental values in [14]. That is, as φ increases from 0.6 to 1.3, the S_Ls of the three fuels first increase and then decrease. However, there is a significant gap between the two curves. In other words, the calculated S_Ls for the three single-component fuels cannot match with the experimental values. Therefore, the second-stage mechanism should be revised.

By analyzing the sensitivity of the base model on S_L at selected operating conditions, the reactions that affect S_L obvious were picked out. These highly sensitive main-chain branching reactions were revised and subsequently several reaction rate constants were also adjusted to improve the prediction. In addition, the two following reactions keeping highly sensitive were also added, based on the detailed discussion shown by Westbrook et al. [29]:

$$\begin{aligned} \mathrm{OH + H = H_2O} \\ \mathrm{CO + OH = H + CO_2} \end{aligned} \quad (1)$$

Any elementary reaction that produces hydrogen (H) radical increases the rate of branch reaction R9. R21 not only increases the production of H, but also affects the destruction of hydroxyl (OH) radical, so these two elementary reactions take vital parts in the autoignition process. Moreover, this stage reduced model cannot predict the reactions related to H accurately. As a result, the parameters of these reactions related to H require revision.

Based on detailed model developed by Mehl et al. [30], some Arrhenius coefficients were adjusted. The elementary reactions associated with H radical may accurately reproduce the characteristics of iso-octane flame, so vital reactions that affect S_L were extracted, as shown below:

$$\begin{aligned} \mathrm{CHCHO = CH3 + CHO} \\ \mathrm{C2H2 + O = HCCO + H} \end{aligned} \quad (2)$$

In addition, OH radical has an obvious effect on autoignition of gasoline-ethanol surrogates [14]; the parameters of the reactions involving H or OH in the products or reactants should be subjected to sensitivity analysis, and then the kinetics of the vital reactions need to be adjusted.

As a result, the final model including 278 species and 1439 reactions was proposed. To determine the prediction accuracy of this model, S_Ls of the three initial fuel components were calculated. Figure 2(b) shows the calculated value and the experimental data under different φs. It is obvious that final mechanism can predict S_Ls of the three initial components more accurately than second-stage model. This also indicates that the revision of the model is effective.

4.2. Pressure and Heat Release Rate. To further study the oxidation process of gasoline-ethanol surrogates in the HCCI engine, in-cylinder pressure (*P*) and heat release rate (*HRR*) in HCCI mode were calculated by coupling CHEMKIN with CFD software. The given HCCI operating conditions were as follows: $n = 1200$ r/min, $P_{in} = 0.1$ MPa, $T_{\mathrm{in}} = 423$ K, and different φs ($\varphi = 0.25$, 0.30, 0.35, 0.40).

The HCCI combustion chamber model based on HCCI engine parameters is given in Figure 3.

Coupling CHEMKIN with CFD, calculated values and experimental results for in-cylinder pressures and *HRR*s were compared, when $P_{in} = 0.1$ MPa, $n = 1200$ r/min, $\varphi = 0.25$, 0.3, 0.35, 0.4, as shown in Figure 4.

As can be seen from Figure 4, curves of experimental values and the calculated data show the same trend. Firstly, under the above conditions, when equivalent ratio φ rises, the two peak values of *P* and *HRR* obtained by simulation show an increasing trend, and the corresponding timing of the peak value is advanced. Obviously, variation trend of the two parameters (*P* and *HRR*) obtained by simulation is consistent with the experimental data. Secondly, the calculated data are in good agreement with the experimental values.

P rises slightly as the piston moves up. After autoignition, *P* rises sharply until it reaches the peak in-cylinder pressure ($P_{\max}$), and then *P* gradually decreases as the piston moves down during the power stroke. Inevitably, there are two factors that may cause the predicted *P*s to be higher than the experimental values. Firstly, the calculation is performed by a zero-dimensional model that ignores crevices and the inhomogeneity of mixture concentration and temperature in the cylinder. Secondly, the assumptions are closed, constant volume and adiabatic.

In addition, when T_{in} rises from 413 K to 433 K, the formation and combustion e are speed up, the formation of OH and related active groups are accelerated, so the ignition delay is shortened. However, the $P_{\max}$ at high T_{in} (433 K) is smaller than that at low temperature (413 K). This is because T_{in} is too high, resulting in a reduction in the density of the mixture, which in turn reduces the quantity of injection fuel per cycle.

4.3. Heat Release Rate. The calculated *HRR* at two different φs (0.3, 0.4) using this model and the model by Li et al. [16] are compared with HCCI experimental data in Figures 5(a) and 5(b).

The given conditions were $P_{in} = 0.1$ MPa, $T_{in} = 433$ K and $n = 1200$ r/min.

The simulation curve (blue line) obtained in this study follows the trend: when φ increases, the heat release

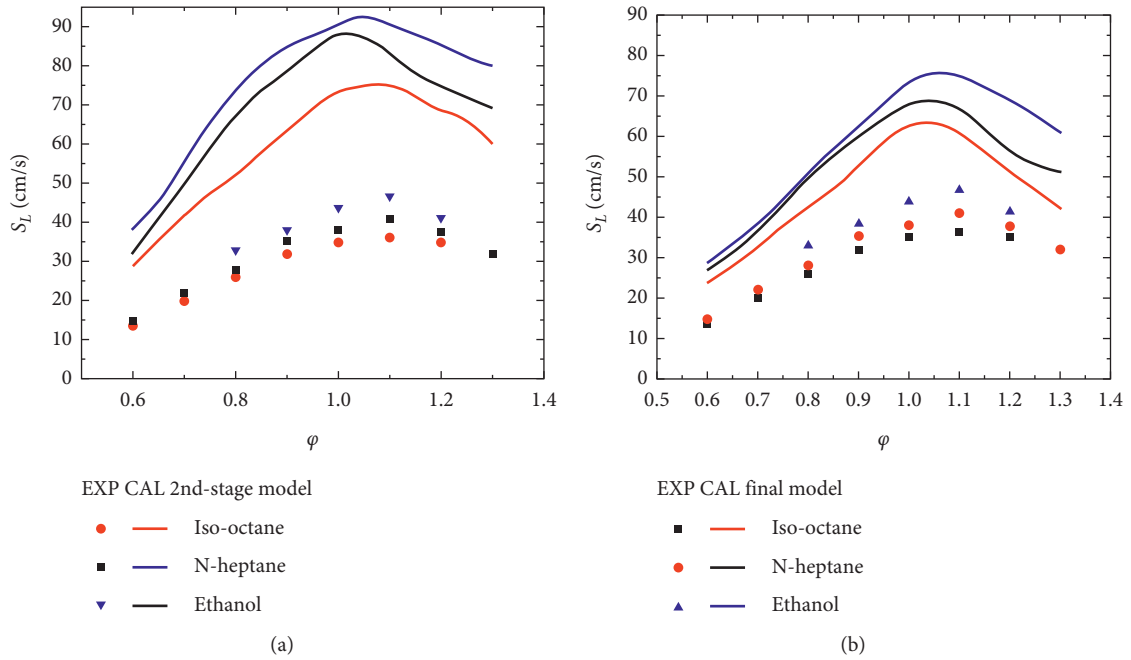

Figure 2: S_Ls for the calculated data and experimental values under different φs: (a) predictions of the second-stage model; (b) predictions of the final model.

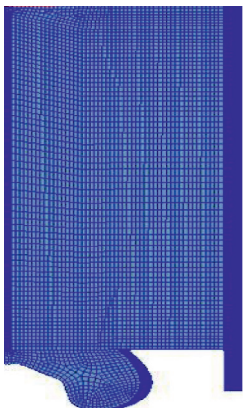

Figure 3: HCCI combustion chamber 3D-CFD model.

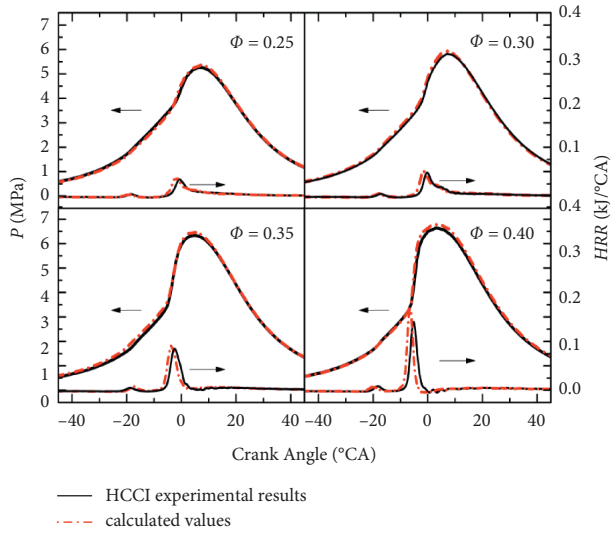

Figure 4: Calculated values and experimental results for P and HRR.

in the cylinder is more concentrated, and the shape of the HRR curve will change to a narrow and high trend. That is, when φ increases, the peak heat release rate increases accordingly, and the time of occurrence is advanced. This is mainly because, as φ increases, the number of activated molecules increases and the thermal energy in the cylinder is more sufficient, which not only leads to faster overall reaction, shorter ignition delay period, and concentrated heat release, but also increases the heat release in the cylinder.

Due to the inhomogeneity, the HRRs calculated by this model and the model of Li et al. [16] are significantly greater than the HCCI experimental data. As mentioned earlier, for the same reasons, the calculated Ps are also higher than the experimental results.

Above all, the predicted trends using this model are in consistency with the HCCI experimental results.

4.4. CA10 and CA50. In engine experimental research, τ is the duration from the opening of the injector needle valve until the moment when the P curve starts to separate from the pure compression curve at the compression process. This moment when P rises sharply refers to the CA corresponding to the heat release percentage being 10% ($CA10$). Moreover, when 50% of the heat has been released is usually considered as the midpoint of the combustion process per engine cycle, which was marked as $CA50$.

To further study the oxidation process in HCCI cylinder, $CA10$s and $CA50$s at different T_{in}s by using the final model, the HCCI results are compared in Figures 6 and 7. As can be

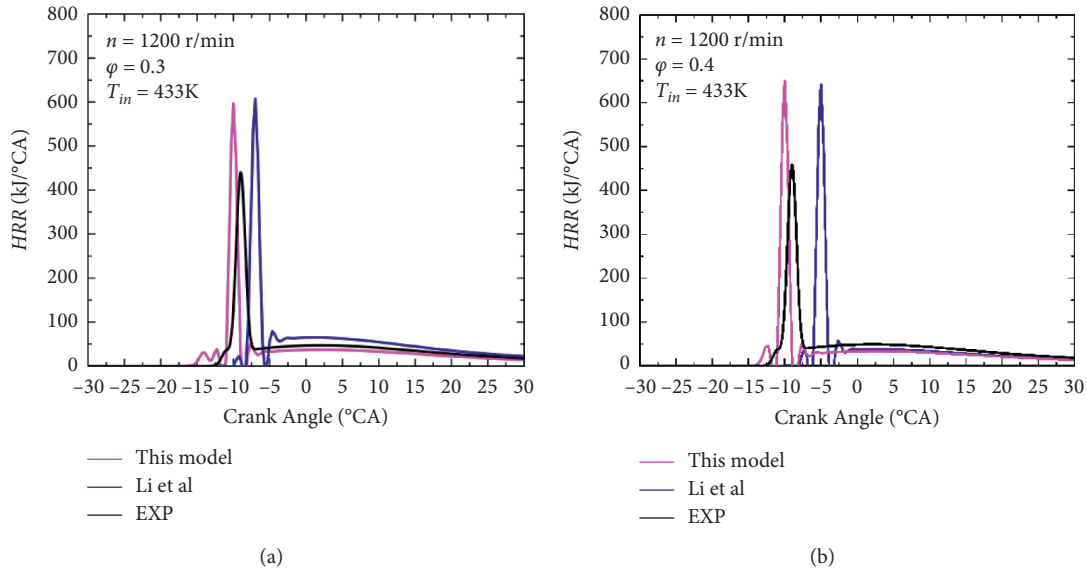

Figure 5: Comparison of the HCCI experimental and calculated HRRs as functions of CA at $P_{in} = 0.1$ MPa, $T_{in} = 433$ K, $n = 1200$ r/min, and two different φs: (a) $\varphi = 0.3$, (b) $\varphi = 0.4$.

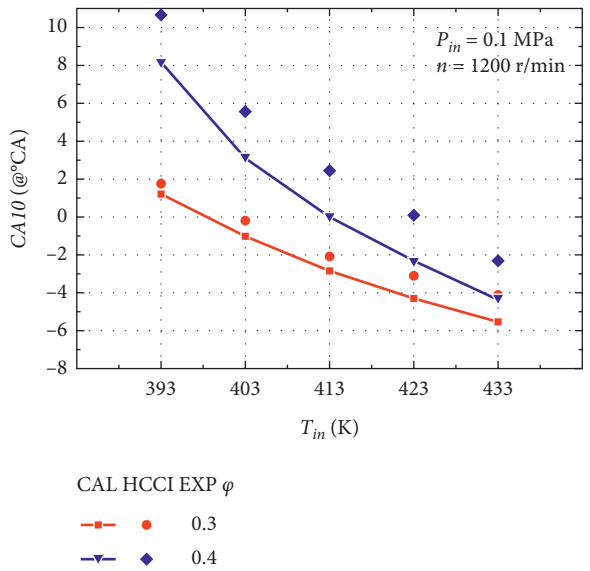

Figure 6: HCCI experimental CA10s and calculated results under different T_{in}s, when $P_{in} = 0.1$ MPa, $n = 1200$ r/min.

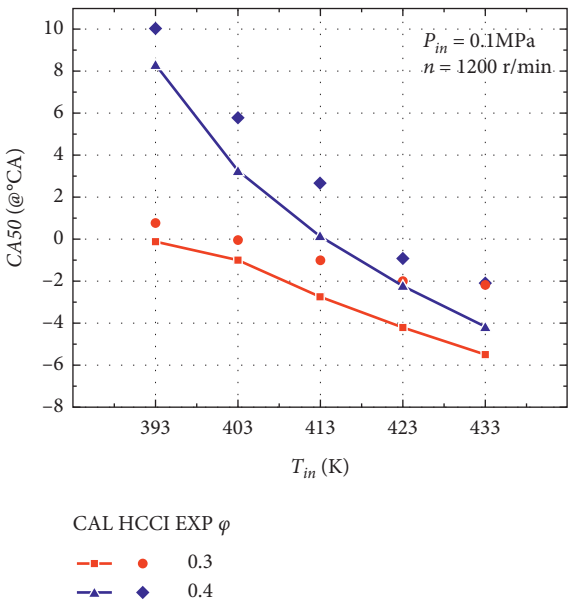

Figure 7: HCCI experimental CA50s and predictions under different T_{in}s, when $P_{in} = 0.1$ MPa and $n = 1200$ r/min.

seen from Figure 6, when T_{in} decreases from 433 K to 393 K, *CA10* is in advance about 6°CA ~12°CA. Figure 7 shows that the midpoint of combustion process (*CA50*) at T_{in} of 393 K is 6°CA ~12°CA later than at T_{in} of 433 K.

Above all, the results indicate that T_{in} play a vital part in oxidation process of the test fuel. Good agreements can be achieved between the calculation and the experimental data.

Comparison of the experimental data (scatters) [31] and calculated results (lines) for PRF100/PRF90/PRF0 in a rapid compression machine (RCM) can be seen in Figure 8. It shows the relationship between τ and φ. As expected, the higher the proportion of n-heptane in PRFs is, the shorter the τ is.

Moreover, the higher T_{in} and the higher T during the compression stroke cause the mixture to be more homogeneous. As a result, more active radicals may be generated and the reaction rate may be accelerated, which lead to a shorter τ.

Overall, a higher intake air temperature will advance the phase of the peak heat release rate, which means that the heat release of the fuel in the HCCI cylinder will be more concentrated; that is, when T_{in} is appropriately increased, *CA10* and *CA50* advanced and the *HRR* curve tends to be narrow and high.

4.5. Mole Fractions of the Vital Species. Comparison of the predicted mole fractions for iso-octane, heptane, and ethanol by our developed model and Li et al. model [16] at different T_{in}s can be seen in Figure 9.

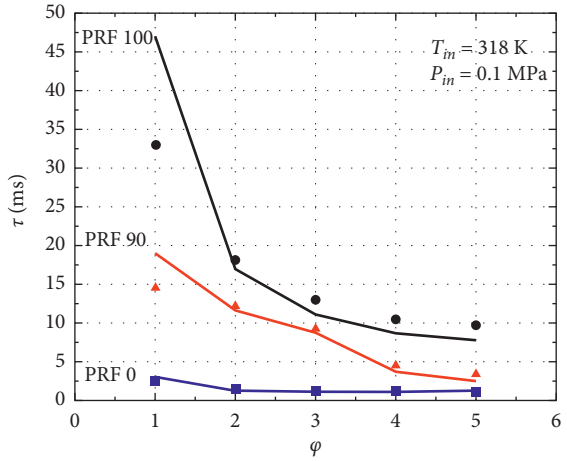

Figure 8: Comparison of experimental τ [31] in RCM and modeling results.

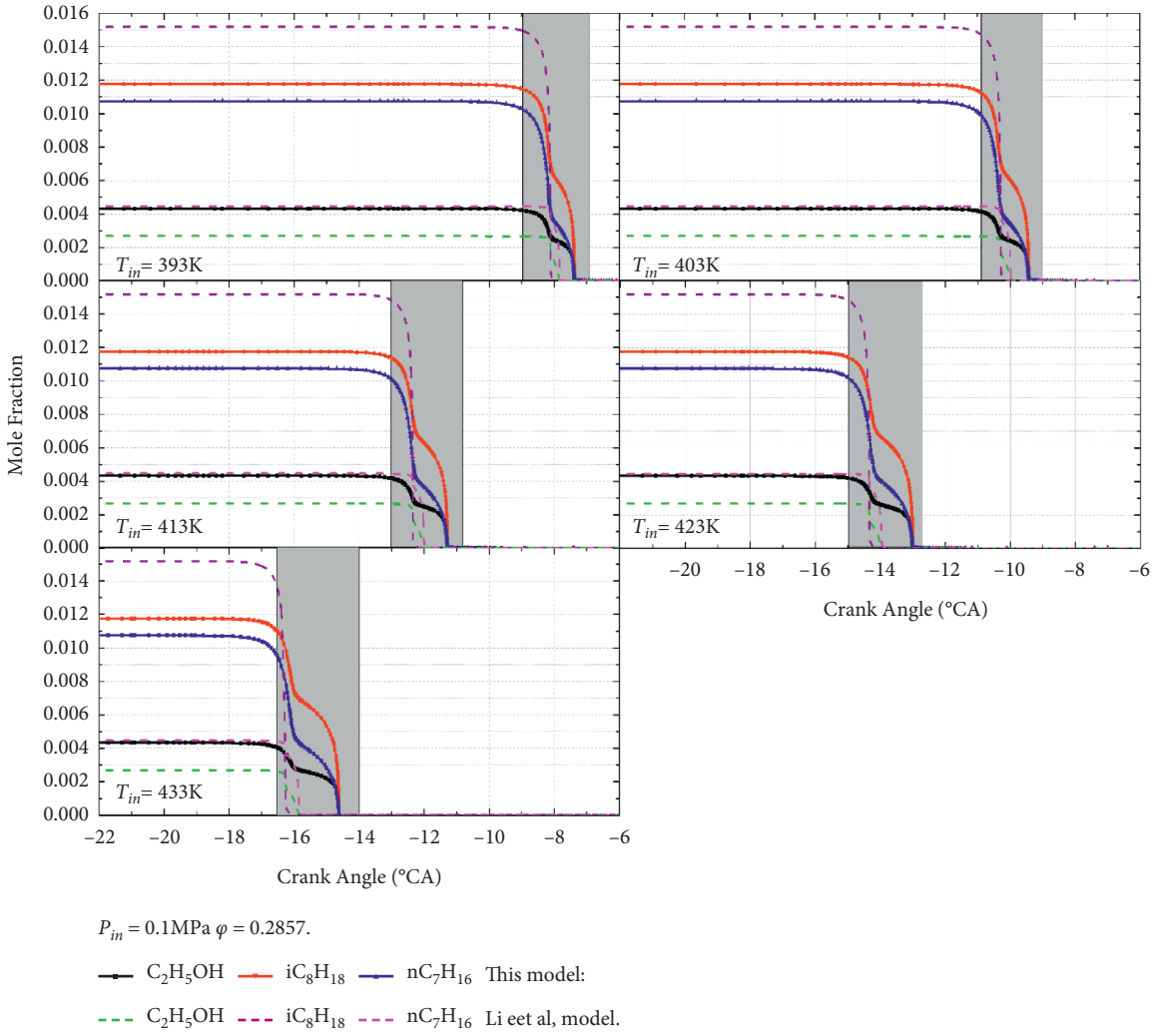

Figure 9: Mole fractions of iso-octane, heptane, and ethanol predicted by our developed model and Li et al. model [16] at different T_{in}s.

The following findings can be drawn from Figure 9. Firstly, under the same operating condition, the moments at which the three initial components begin to decrease sharply predicted by the two models are relatively close, as shown by the shaded area in Figure 9. This indicates that the τs predicted by the two mechanisms are roughly the same. Secondly, when T_{in} increases from 393 K to 433 K, the moments at which the three initial components begin to

decrease sharply are advanced from −8°CA to −14°CA. This is because the formation of free radicals may be accelerated at high T_{in}, thus leading to the advance of autoignition.

In summary, the final model is predictive at the autoignition phase by comparing the predicted τ, P, S_L, *HRR*, T, *CA10*, *CA50*, and mole fractions of vital species under selected conditions.

5. Conclusions

This work developed a mechanism (278 species, 1439 reactions) for gasoline-ethanol surrogates by implementing the reduction and merge scheme. DRGEP and QSSA methods were used to efficiently reduce the mechanism. Moreover, the kinetic parameters of the relevant reactions related to the formation and consumption of H and OH were adjusted.

HCCI experiments were conducted on the combustion of gasoline-ethanol surrogates. More HCCI experimental data were provided to validate the models for the oxidation.

The proposed mechanism was validated as well as the predictions of the previous literature model. Since the calculation is based on ideal assumptions, there is a gap between the simulated curve and the experimental curve. Overall, the prediction of this developed model was found satisfactory in terms of certain characteristic parameters involving S_L, P, T, *CA10*, *CA50*, τ, *HRR*, and mole fractions of species under the selected HCCI conditions.

Based on the reduced mechanism and HCCI engine model developed in this paper, we will further analyze the influence of other boundary conditions (such as intake pressure, engine speed, and EGR rate) on the flame structure and combustion flow field of fuel combustion in the future.

Nomenclature

CA10: Timing at which 10% of the heat has been released (@oCA)
CA50: Crank angle at which 50% of the heat has been released (@oCA)
T_{in}: Intake temperature (K)
φ: Equivalence ratio

Abbreviation

BTDC: Before top dead center
CFD: Computational fluid dynamics
TRF: Toluene primary reference fuel.

Data Availability

No data were used to support this study.

Conflicts of Interest

The authors declare that there are no conflicts of interest regarding the publication of this paper.

Acknowledgments

This study was supported by the Special Fund Chang'an University (300102228509, 300102228403, 300102228505, 300102229502, and 300102229202).

References

[1] M. P. Halstead, L. J. Kirsch, and C. P. Quinn, "The autoignition of hydrocarbon fuels at high temperatures and pressures-fitting of a mathematical model," *Combustion and Flame*, vol. 30, pp. 45–60, 1977.
[2] R. A. Cox and J. A. Cole, "Chemical aspects of the autoignition of hydrocarbon-air mixtures," *Combustion and Flame*, vol. 60, no. 2, pp. 109–123, 1985.
[3] H. L. Li, D. L. Miller, and N. P. Cernansky, "Development of a reduced chemical kinetic model for prediction of preignition reactivity and autoignition of primary reference fuels," in *Proceedings of the SAE World Congress & Exhibition*, April 1996.
[4] S. Tanaka, F. Ayala, and J. C. Keck, "A reduced chemical kinetic model for HCCI combustion of primary reference fuels in a rapid compression machine," *Combustion and Flame*, vol. 133, no. 4, pp. 467–481, 2003.
[5] N. A. Slavinskaya and O. J. Haidn, "Modeling of n-heptane and iso-octane oxidation in air," *Journal of Propulsion and Power*, vol. 19, no. 6, pp. 1200–1216, 2003.
[6] H. J. Curran, W. J. Pitz, C. K. Westbrook, G. V. Callahan, and F. L. Dryer, "Oxidation of automotive primary reference fuels at elevated pressures," *Symposium (International) on Combustion*, vol. 27, no. 1, pp. 379–387, 1998.
[7] Y. Ra and R. D. Reitz, "A reduced chemical kinetic model for IC engine combustion simulations with primary reference fuels," *Combustion and Flame*, vol. 155, no. 4, pp. 713–738, 2008.
[8] P. Kirchen, M. Shahbakhti, and C. R. Koch, "A skeletal kinetic mechanism for PRF combustion in HCCI engines," *Combustion Science and Technology*, vol. 179, no. 6, pp. 1059–1083, 2007.
[9] N. M. Marinov, "A detailed chemical kinetic model for high temperature ethanol oxidation," *International Journal of Chemical Kinetics*, vol. 31, no. 3, pp. 183–220, 1999.
[10] Y. D. Liu, M. Jia, M. Z. Xie, and B. Pang, "Development of a new skeletal chemical kinetic model of toluene reference fuel with application to gasoline surrogate fuels for computational fluid dynamics engine simulation," *Energy & Fuels*, vol. 27, no. 8, pp. 4899–4909, 2013.
[11] H. Wang, M. Yao, Z. Yue, M. Jia, and R. D. Reitz, "A reduced toluene reference fuel chemical kinetic mechanism for combustion and polycyclic-aromatic hydrocarbon predictions," *Combustion and Flame*, vol. 162, no. 6, pp. 2390–2404, 2015.
[12] S. Jerzembeck, A. Sharma, and N. Peters, "Laminar burning velocities of nitrogen diluted standard gasoline-air mixture," in *Proceedings of the SAE World Congress & Exhibition*, June 2008.
[13] D. Zheng and B. J. Zhong, "Chemical kinetic model for ignition of three-component fuel comprising iso-Octane/n-Heptane/Ethanol," *Acta Physico-Chimica Sinica*, vol. 28, no. 9, pp. 2029–2036, 2012.
[14] B.-J. Zhong and D. Zheng, "Chemical kinetic mechanism of a three-component fuel composed of iso-octane/n-heptane/ethanol," *Combustion Science and Technology*, vol. 185, no. 4, pp. 627–644, 2013.

[15] R. Lemaire, E. Therssen, and P. Desgroux, "Effect of ethanol addition in gasoline and gasoline-surrogate on soot formation in turbulent spray flames," *Fuel*, vol. 89, no. 12, pp. 3952–3959, 2010.
[16] Y. Li, A. Alfazazi, B. Mohan et al., "Development of a reduced four-component (toluene/n-heptane/iso-octane/ethanol) gasoline surrogate model," *Fuel*, vol. 247, no. 1, pp. 164–178, 2019.
[17] M. Sjoberg and J. E. Dec, "An investigation into lowest acceptable combustion temperatures for hydrocarbon fuel in HCCI engines," *Proceedings of the Combustion Institute*, vol. 30, no. 2, pp. 2719–2726, 2004.
[18] M. Sjoberg and J. E. Dec, "Isolating the effects of fuel chemistry on combustion phasing in an HCCI engine and the potential of fuel stratification for ignition control," in *Proceedings of the SAE World Congress & Exhibition*, Chicago, IL, USA, June 2004.
[19] J. Park, Z. F. Xu, and M. C. Lin, "A computational study of the kinetics and mechanism for the C2H3 + CH3OH reaction," *International Journal of Chemical Physics*, vol. 47, no. 12, pp. 764–772, 2003.
[20] S. Xu and M. C. Lin, "Theoretical study on the kinetics for OH reactions with CH3OH and C2H5OH," *Proceedings of the Combustion Institute*, vol. 31, no. 1, pp. 159–166, 2007.
[21] Z. F. Xu, J. Park, and M. C. Lin, "Thermal decomposition of ethanol. III. A computational study of the kinetics and mechanism for the CH3+C2H5OH reaction," *The Journal of Chemical Physics*, vol. 120, no. 14, pp. 6593–6599, 2004.
[22] C.-W. Wu, Y.-P. Lee, S. Xu, and M. C. Lin, "Experimental and theoretical studies of rate coefficients for the reaction O(3P) + C2H5OH at high temperatures," *The Journal of Physical Chemistry A*, vol. 111, no. 29, pp. 6693–6703, 2007.
[23] M. Fikri, J. Herzler, R. Starke, C. Schulz, P. Roth, and G. T. Kalghatgi, "Autoignition of gasoline surrogate mixtures at intermediate temperatures and high pressures," *Combustion and Flame*, vol. 152, no. 1-2, pp. 276–281, 2008.
[24] J. B. Heywood, *A Textbook for Internal Combustion Engines Fundamentals*, McGraw-Hill Science/Engineering/Math, New York, NY, USA, 1988.
[25] C. Zhang and H. Wu, "Combustion characteristics and performance of a methanol fueled homogenous charge compression ignition (HCCI) engine," *Journal of the Energy Institute*, vol. 89, no. 3, pp. 346–353, 2016.
[26] Y. Chen, M. Mehl, Y. Xie, and J.-Y. Chen, "Improved skeletal reduction on multiple gasoline-ethanol surrogates using a Jacobian-aided DRGEP approach under gasoline compression ignition (GCI) engine conditions," *Fuel*, vol. 210, pp. 617–624, 2017.
[27] E. A. Tingas, D. J. Diamantis, and D. A. Goussis, "Issues arising in the construction of QSSA mechanisms: the case of reduced n-heptane/air models for premixed flames," *Combustion Theory and Modelling*, vol. 6, no. 22, pp. 1049–1083, 2018.
[28] J. C. G. Andrae, T. Brinck, and G. T. Kalghatgi, "HCCI experiments with toluene reference fuels modeled by a semi-detailed chemical kinetic model," *Combustion and Flame*, vol. 155, no. 4, pp. 696–712, 2008.
[29] C. K. Westbrook, Y. Mizobuchi, T. J. Poinsot, P. J. Smith, and J. Warnatz, "Computational combustion," *Proceedings of the Combustion Institute*, vol. 30, no. 1, pp. 125–157, 2005.
[30] M. Mehl, T. Faravelli, E. Ranzi, D. Miller, and N. Cernansky, "Experimental and kinetic modeling study of the effect of fuel composition in HCCI engines," *Proceedings of the Combustion Institute*, vol. 32, no. 2, pp. 2843–2850, 2009.
[31] S. Tanaka, F. Ayala, J. C. Keck, and J. B. Heywood, "Two-stage ignition in HCCI combustion and HCCI control by fuels and additives," *Combustion and Flame*, vol. 132, no. 1-2, pp. 219–239, 2003.